

Proceedings of the SPIE'S 1993 Symposium on  
Aerospace and Remote Sensing, April 12-16, 1993,  
Marriott Orlando World Center, Orlando, Florida, U.S.A.

Multiple sensor data integration for space operations

Marie France Collin, Kumar Krishen ✓  
NASA Johnson Space Center  
Houston, TX, 77058

Roland Pesty  
ITMI  
61, Chemin du Vieux Chene  
38244 Meylan Cedex, France

ABSTRACT

Adaptive and intelligent multisensor perception is a characteristic that will be needed for Space Robotics and Automation Systems in order to improve productivity and flexibility. However, one of the major technical difficulties is related to illumination conditions in space. Space robotic systems, whether autonomous or not, will have to evolve and operate in a wide variety of illumination conditions within their mission: night, deep shadows, high illumination, or specularities. These robotic systems will also have to perceive and recognize the reflectance and emittance properties of a wide variety of rough surfaces. The purpose of our current research is to study a multisensor perception system that will be able: (1) to adapt the sensing strategy to the lighting conditions and (2) to allow for the geometrical and physical analysis of the surface properties on the scene.

INTRODUCTION

The settlement of a lunar outpost will include a wide variety of robotic missions such as surface exploration; system monitoring for maintenance; and mining for construction purposes. The achievement of these operations, either partially or completely automated, requires advanced remote sensing technologies to assure the perception of the lunar scene at any time and at any location. The technologies should also provide a description of the surface in terms of properties such as roughness, dielectric constant, emissivity, reflectivity, orientation, and slopes. This full description is needed for safe navigation and object recognition during the mission operations. To meet these requirements, a new approach for sensing, integrating, and interpreting remotely-sensed data has been investigated and is being developed. The involved sensors include visible, infrared, microwave, and millimeter wave sensors.

Initially, this paper presents the physical reflectance and emittance models which are the theoretical basis of the multisensor integration method. Then, from the physical model analysis, the sensor sensitivities to surface roughness and dielectric constant are discussed. This leads to a multisensor integration method allowing the perception of these surface properties; an approach that has been developed and tested using simulated data. The preliminary results are presented in the case of a simulated lunar environment.

1. PHYSICAL MODELS

Perception models have been developed and used in the field of remote sensing for earth observation purposes.<sup>1,2,3,4</sup> These models consider two types of processes which result from the perception of the scattered/reflected and emitted radiations.

## 1.1 Reflection models

The energy reflected off a surface and received by a remote sensing device is related to a scattering coefficient ( $\sigma_{pq}$ ), depending on the surface physical properties and especially on roughness, orientation, and dielectric constant, in a decreasing order of importance. The subscript pq indicates that the transmitted field is p-polarized and the received field is q-polarized. In the past, several reflection models have been derived, depending on the frequency range of illumination and on the surface geometry. The most widely used models are the specular model (or Kirchhoff approximation) for locally smooth surfaces, the Small Perturbation Model (SPM) for slightly rough surfaces, and the Lambertian model for rough surfaces.

Typical reflected power (in dB) for each of these three models is presented in figures 1, 2, and 3 as a function of the illumination incidence angle and for the same value of the dielectric constant ( $\epsilon$ ). In these models, the roughness of the surface is normalized with respect to the illumination wavelength ( $\lambda$ ). The normalized roughness parameters are:  $r = k \sigma$ , and  $p = k l$ , where  $k$  is the wave number, defined as  $2\pi/\lambda$ ,  $\sigma$  is the standard surface height deviation, and  $l$  is the surface height correlation length.

The approximate roughness ranges for the validity of each model are summarized in the following table.

Model	roughness parameters
Kirchhoff	$k\sigma < 0.17$ , $kl > 6$
SPM	$k\sigma < 0.3$ , $kl < 3$ .
Lambertian	$k\sigma > 1$ .

For rough surfaces (Lambertian model), the reflected power is spread in all directions, whereas for smooth surfaces (Kirchhoff model), the surface behaves like a perfect mirror and the reflected power is mainly concentrated in the specular direction. The SPM model has both specular and diffuse components.

## 1.2 Emission models

Emission models are the governing models for passive sensors such as infrared sensors and radiometers (passive microwave sensing). The spectral brightness ( $B_f$ ) perceived by a thermal sensor is related to the physical temperature ( $T$ ) of the surface and to its emissivity as formulated by Planck's radiation law. To simplify analysis of the emitted radiations, the theoretical models are divided into two categories: the high frequency model and the low frequency model. In the case of the low frequency model, which is valid for passive microwave sensors, the power emitted by the surface increases with the surface temperature. Therefore, a radiometer provides a brightness temperature measurement ( $T_b$ ), depending on the surface parameters, and defined as:

$$T_b(\theta, p) = E(\theta, p) T$$

where  $\theta$  is the observation angle,  $p$  is the polarization state of the radiometer, and  $T$  is the physical temperature of the surface.

At high frequencies, Planck's radiation law reduces to the following:

$$T_b(\theta, p) = E(\theta, p) \frac{2\pi h f^5}{c^3} \exp^{-hf/kT}$$

where  $h$ ,  $f$ ,  $c$ ,  $k$  and  $T$  are the Planck's constant, the frequency, the velocity of light, the Boltzmann's constant, and the physical temperature respectively. Emissivity,  $E(\theta, p)$ , is adequately modeled by a Lambertian law for any surface type, according to the dielectric constant of the surface. In that case,

emissivity does not vary considerably with the observation angle. The emitted intensity is therefore a function of the physical temperature and dielectric constant of the surface, but is independent of the observation angle ( $\theta$ ).

Typical examples of brightness temperature for these two models are shown as a function of the observation angle in figures 4 and 5 for the same value of the dielectric constant ( $\epsilon$ ) and two different roughness parameters.

## 2. KEY SURFACE PARAMETERS

The purpose of this section is to understand to which extent the surface parameters, mainly roughness and dielectric constant, affect the sensor response. This parametric analysis should allow selection of a sensing strategy (sensor, sensor mode, and frequency range) using the sensor configuration that is most sensitive to the required surface parameter.

### 2.1 Roughness

The parameter that has the greatest effect is surface roughness. The roughness affects both the intensity and the shape of the reflection and emission pattern. The higher the roughness, the more diffuse the scattering. The perception of a surface as smooth or rough allows selection of the appropriate scattering and emission model and further analysis of the surface parameters.

From theoretical analysis and experimental observations, the effects of surface roughness on the sensor responses can be summarized as follows:

with active sensors, the cross-polarized return increases as the roughness increases. This follows from figures 1, 2 and 3, where the cross-polarized return is zero for the Kirchhoff model (specular surfaces), very low for the SPM model (slightly rough surfaces), and similar to the direct-polarized return for the Lambert model (very rough surfaces).

with passive sensors, at high observation angles, the difference between perpendicular and parallel polarized radiations is higher for specular returns (low roughness) than for diffuse returns (high roughness). This is verified in figures 4 and 5. The difference between perpendicular and parallel radiations is negligible for all observation angles for the rough surface, and high for the smooth surface.

### 2.2 Dielectric constant

The dielectric constant provides scene interpretation since it allows for distinguishing objects on the basis of their surface material and composition. The dielectric constant affects the sensor response through the Fresnel reflection coefficients. Since the Fresnel coefficient influences both reflection and emission, the dielectric constant will affect both passive and active sensing devices.

The effects of dielectric constant on reflection and emission are as follows:

for all frequencies, the increase of the dielectric constant increases the reflected intensities and decreases the emitted intensities.

the effect of dielectric constant is more sensitive at microwave frequencies than at visible frequencies because of the wider variation of the dielectric constant at low frequencies.

This can be concluded by comparing figures 3 and 6, which show a rough surface with two different values of the dielectric constant.

#### 4. ADAPTIVE MULTISENSING STRATEGY FOR SURFACE PROPERTIES ANALYSIS

From the previous sensor sensitivity analysis, it appears that:

for the perception of surface roughness, the depolarization factor of an active microwave sensor is a reliable indicator. Therefore, the integration of both cross-polarized and direct-polarized microwave responses should provide an estimate of the surface roughness.

for the perception of the dielectric constant of a surface, the integration of passive microwave with an estimation of the surface temperature (using an infrared sensor, for example) should provide an estimate of the dielectric constant as the passive microwave return is related to emissivity, which in turn is sensitive to the dielectric constant.

These multisensor configuration examples have been tested using simulated sensor data. The results are presented in the following section.

#### 5. APPLICATION TO SIMULATED SENSOR DATA

The multisensor integration method has been applied to the simulated lunar environment in order to estimate the surface roughness and dielectric constant. The sensor data has been simulated using the presented reflectance and emittance models.

The result of the integration of the simulated cross-polarized and direct-polarized microwave returns are displayed in figure 7. This multisensor configuration visually reveals the effect of roughness. In this example, the object roughness parameters are  $k_s = 3 \times 10^{-4}$  and  $k_l = 0.3$ , whereas the lunar surface parameters are  $k_s = 5 \times 10^{-2}$  and  $k_l = 0.1$ . The cross-polarized return (represented in blue) is very low for the smooth object.

The result of the infrared and passive microwave sensors, for the same simulated lunar scene, are shown in figure 8. The dielectric constant has the values 6 and 3 for the object and the lunar soil respectively. The higher value of the object dielectric constant appears in green on this display, whereas the lunar soil appears in blue.

#### 6. CONCLUSION

Using simulated sensor data, we have shown that physical surface properties, and especially surface roughness and dielectric constant, can be perceived when selecting suitable multisensory configurations.

The perceived surface parameters allow for further scene interpretation and mission operations control. The next step will be to quantify these surface characteristics using fuzzy logic fusion techniques. Since the perception models are approximate for the radiation phenomena, fuzzy logic techniques will allow the processing of uncertain, incomplete, and ambiguous measurements using simple implementation methods.<sup>5</sup>

#### 7. ACKNOWLEDGMENT

This work has been supported by a NATO post-doctoral grant by DRET (French Ministry of Defense).

## 8. REFERENCES AND BIBLIOGRAPHY

1. P. Beckman, A. Spizzichino, *The Scattering of Electromagnetic Waves from Rough Surfaces*," Pergamon Press, New York, 1963.
2. G.T. Ruck, D.E. Barrick, W. Stuart, C. Krichbaum, *Radar Cross Section Handbook*, Vol. I and II, Plenum Press, New York, 1970.
3. W.H. Peake and T.L. Oliver, "The response of terrestrial surfaces at microwave frequencies," *Report AFAL-TR-70-301*, Wright-Patterson Air Force Base, Ohio, Air Force Avionics Laboratory, May 1971.
4. F.T. Ulaby, R.K. Moore, A. Fung, *Microwave Remote Sensing*, Vol. I, II and III, Artech House, Norwood, MA, 1982.
5. M. F. Collin, K. Krishen, L. H. Pampagnin, "Adaptive Multisensor Fusion For Planetary Exploration Rovers, *paper presented at the Int'l Symposium on Artificial Intelligence, Robotics and Automation in Space (i-SAIRAS)*, Toulouse, France, 1992.

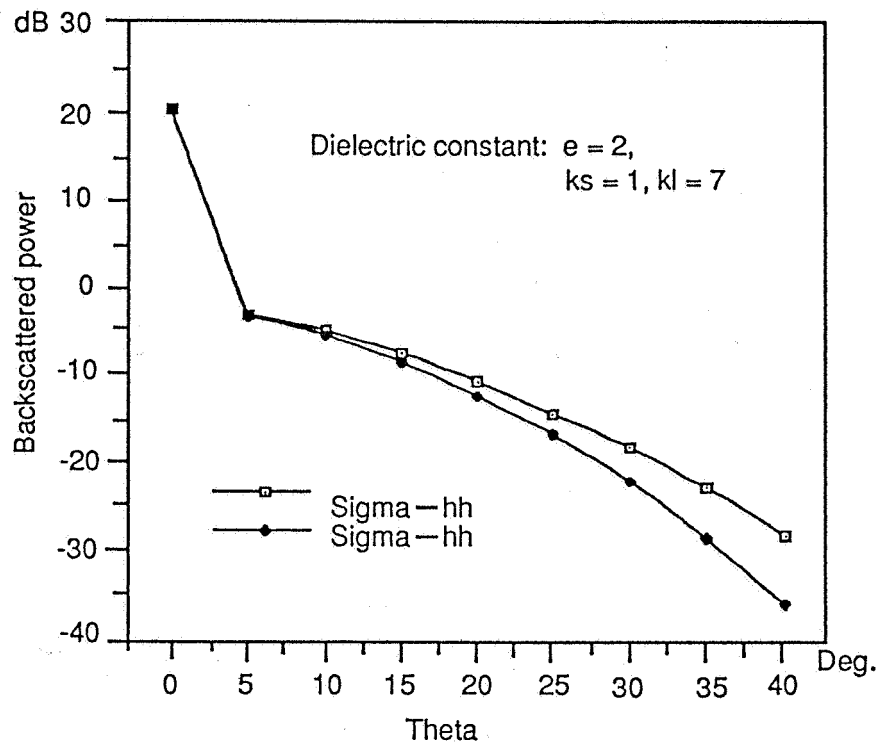


Fig. 1. Typical Kirchhoff reflection

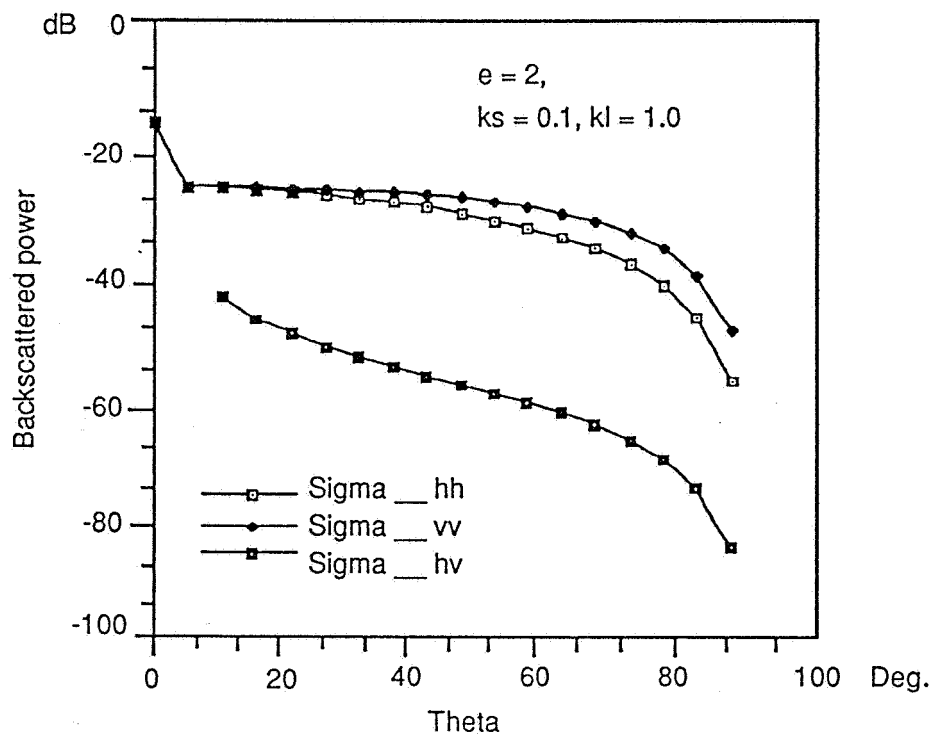


Fig. 2. Typical SPM reflection model.

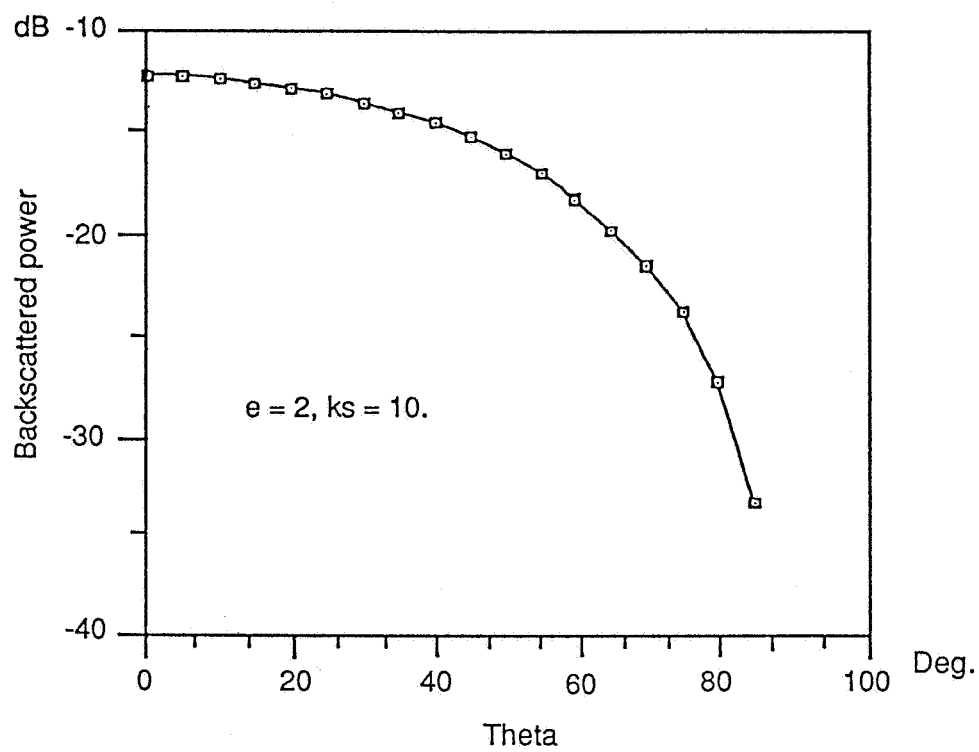


Fig. 3. Typical Lambertian reflection model.

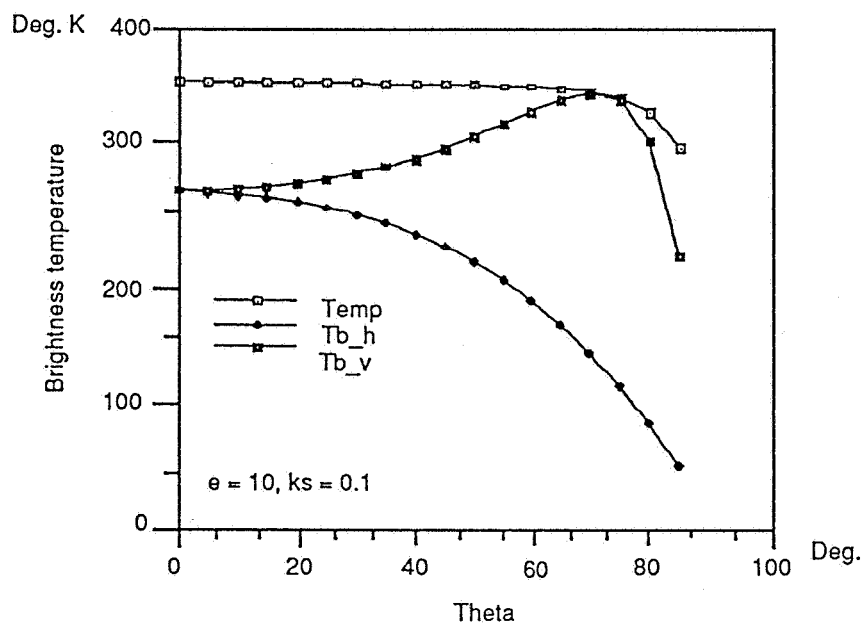


Fig. 4. Typical low frequency emission model.

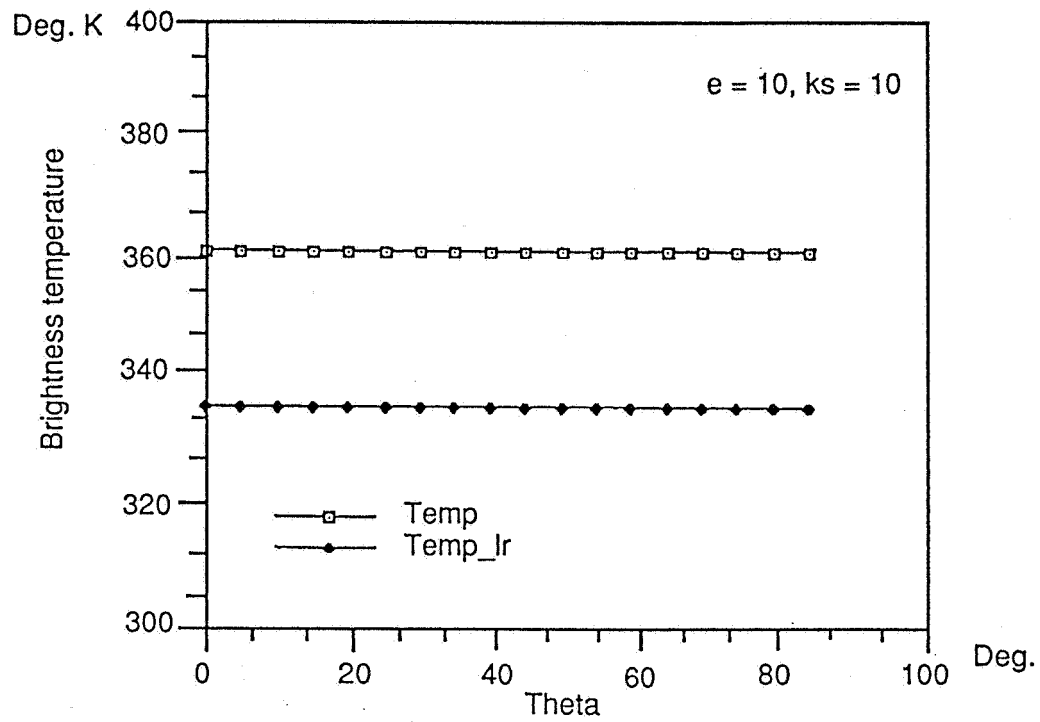


Fig. 5. Typical high frequency emission model.

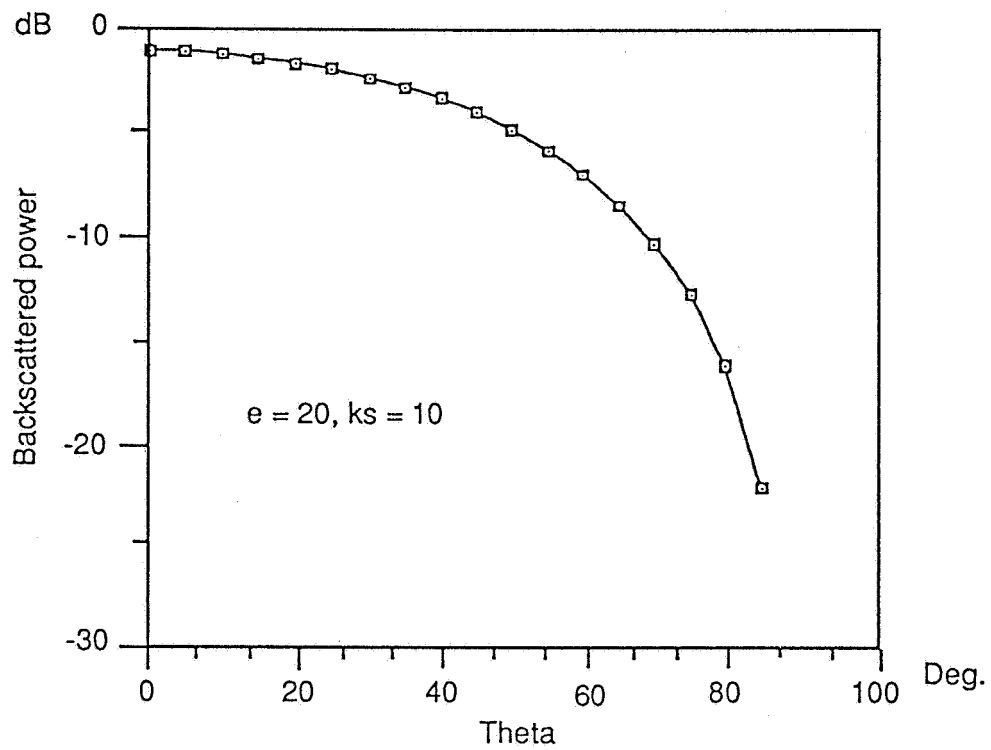
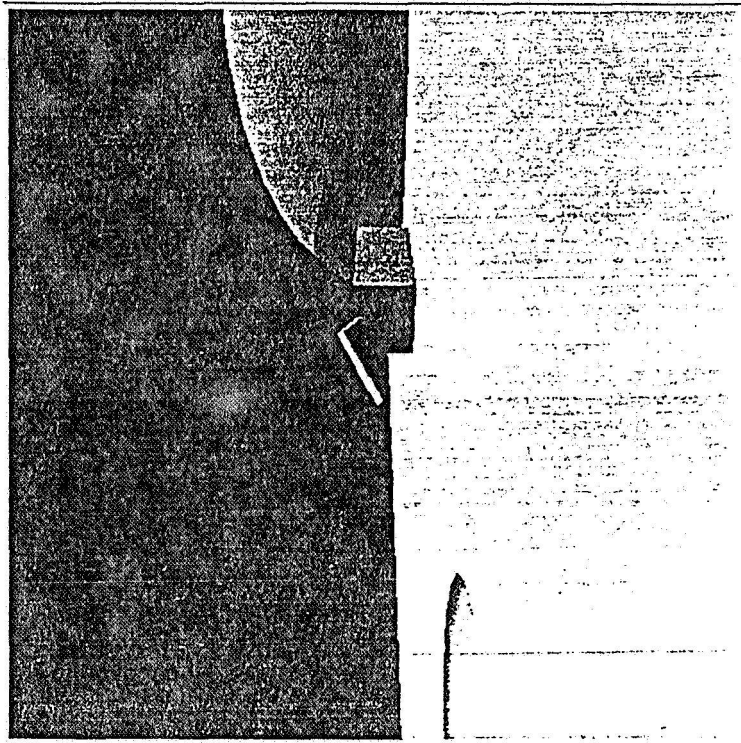


Fig. 6. Lambertian reflection model for a high dielectric constant value.



Lunar Landscape View



1.00    ◀ ▶    Illumination

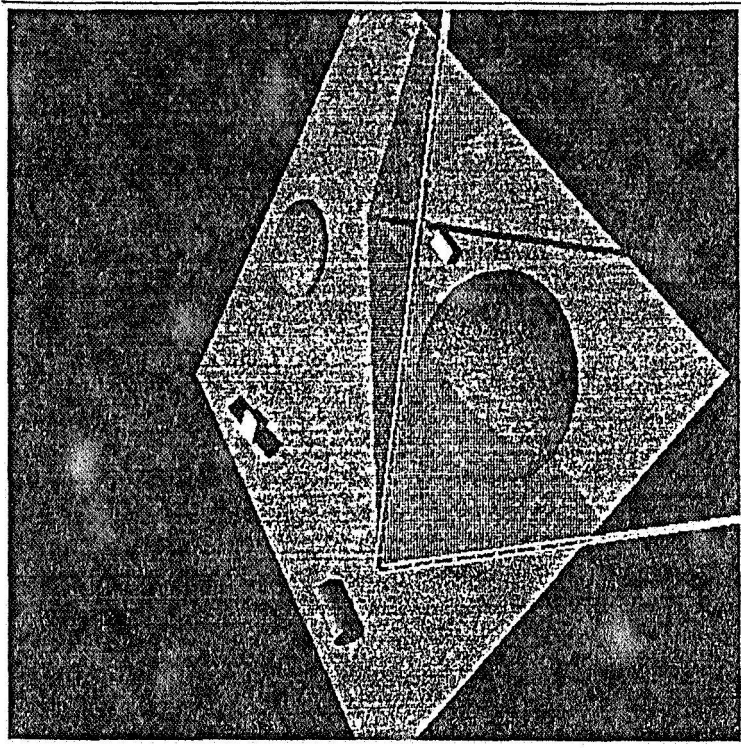
20.44    ◀ ▶    Latitude

40.27    ◀ ▶    Longitude

0.46    ◀ ▶    Time

Execute    High Fidelity    Quit

Nap Sensor View



33.23    ◀ ▶    Sensor Azimuth

0.00    ◀ ▶    Sensor Elevation

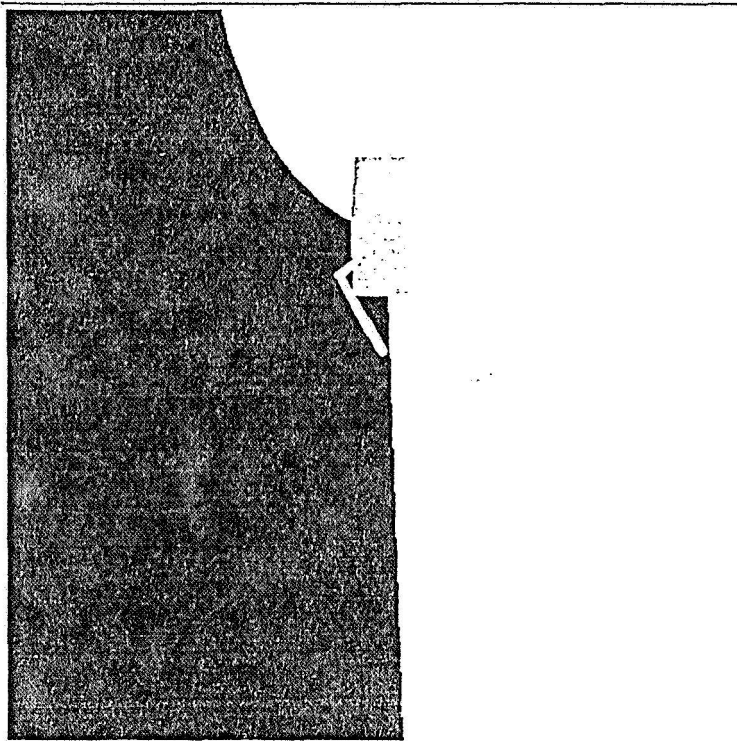
Red:    NULL    mWA1-HH    mWA1-HV

Green:    Visible    Infra-red    Range

Blue:    mWP1-H    mWP1-V    mWP2-H

Fig. 7 Visual perception of surface roughness in a simulated lunar scene

### Lunar Landscape View



### Map Sensor View

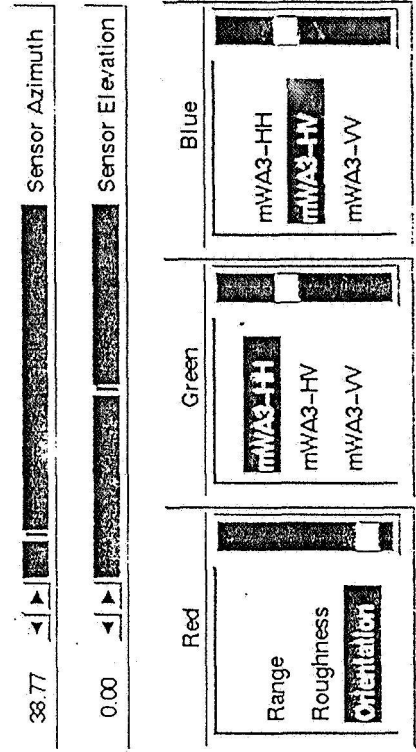
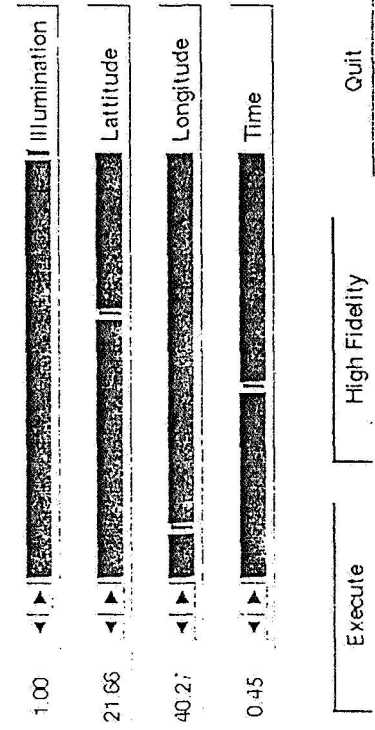
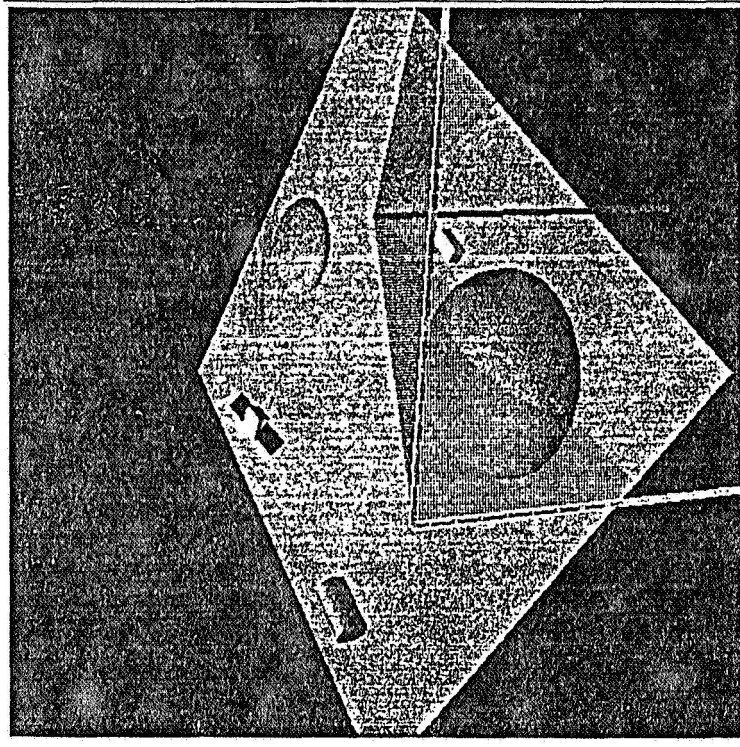


Fig. 8 Visual perception of surface dielectric constant in a simulated linear cone